rich2/cjf-cjfas/cjf-cjfas/cjf99914/cjf0845d14z | xppws | S=3 | 12/16/16 | 7:26 | 4/Color Fig: F1,F4 | Art: **cjfas-2016-0247** | Input-1st disk, 2nd ??

Pagination not final (cite DOI) / Pagination provisoire (citer le DOI)

1

NRC Research Press

RAPID COMMUNICATION

Scalable population estimates using spatial-stream-network (SSN) models, fish density surveys, and national geospatial database frameworks for streams

Daniel J. Isaak, Jay M. Ver Hoef, Erin E. Peterson, Dona L. Horan, and David E. Nagel

Abstract: Population size estimates for stream fishes are important for conservation and management, but sampling costs limit the extent of most estimates to small portions of river networks that encompass 100s–10 000s of linear kilometres. However, the advent of large fish density data sets, spatial-stream-network (SSN) models that benefit from nonindependence among samples, and national geospatial database frameworks for streams provide the components to create a broadly scalable approach to population estimation. We demonstrate such an approach with density surveys for different trout species from 108 sites in a 735 km river network. Universal kriging was used to predict a continuous map of densities among survey locations, and block kriging (BK) was used to summarize discrete map areas and make population estimates at stream, river, and network scales. The SSN models also accommodate covariates, which facilitates hypothesis testing and provides insights about factors affecting patterns of abundance. The SSN–BK population estimator can be applied using free software and geospatial resources to develop valuable information at low cost from many existing fisheries data sets.

Résumé : Les estimations de la taille des populations pour les poissons de cours d'eau sont importantes pour la conservation et la gestion, mais les coûts de l'échantillonnage limitent l'étendue de la portée de ces estimations à de petites portions de réseaux hydrographiques qui comptent des centaines à des dizaines de milliers de kilomètres linéaires. L'arrivée de grandes bases de données sur la densité de poissons, les modèles spatiaux de réseaux de cours d'eau (SSN) qui tirent avantage de la non-indépendance entre échantillons et des cadres nationaux de bases de données géospatiales pour les cours d'eau fournissent toutefois les composantes nécessaires pour élaborer une approche échelonnable d'estimation des populations. Nous faisons la démonstration d'une telle approche à l'aide d'évaluations de la densité de truites de 108 emplacements dans un réseau hydrographique de 735 km. Le krigeage universel est utilisé pour prédire une carte continue des densités dans les lieux évalués et le krigeage par bloc (BK) est utilisé pour résumer des zones cartographiées discrètes et établir des estimations de la population aux échelles du cours d'eau, de la rivière et du réseau. Les modèles SSN peuvent également incorporer des covariables, ce qui facilite les tests d'hypothèse et fournit de l'information sur les facteurs qui influencent les motifs d'abondance. L'estimateur de population SSN-BK peut être appliqué en utilisant des logiciels et des ressources géospatiales gratuits pour produire à faible coût des renseignements utiles à partir de nombreux ensembles de données existants sur des ressources halieutiques. [Traduit par la Rédaction]

Introduction

Answering the question "How many fish live in that stream, river, or lake?" is of fundamental importance to fisheries management and species conservation efforts. Estimation methods addressing that question form an extensive literature, and many sampling techniques have been developed to collect data sets for use with estimators (Hilborn and Walters 1992; Zale et al. 2013). In lotic systems, fish are often sampled by electrofishing, angling, or snorkeling (Dunham et al. 2009), and population estimates are obtained for short reaches of stream using mark–recapture (Petersen 1896; Lincoln 1930) or depletion–removal estimators (Zippin 1958). For nest-building species like salmon and trout, it is also common to conduct visual surveys during the spawning season and use nest counts as a density index or measure of population size (Al-Chokhachy et al. 2005; Falke et al. 2013). Collectively, those estimates form the core data sets that state and federal management agencies use to monitor the status and trends of many

species and fisheries throughout North America and Europe. Thousands of stream and river sites have been sampled in previous decades to estimate local population sizes (Wenger et al. 2011; Meyer et al. 2013; Millar et al. 2016), and as these databases grow, so too do opportunities to mine them for novel information (Isaak et al. 2014).

What is considered a "population" when applying traditional estimators to short sections of stream rarely matches the spatial scales at which habitats are occupied by reproducing populations. Most reproducing populations of stream fishes occupy a wide range of habitat (<1 to 10s of network kilometers) and are affected by natural gradients and anthropogenic stressors occurring over similar scales (Schlosser 1991). The mismatch between measurement scale and biological reality lies at the heart of the Riverscapes paradigm articulated by Fausch et al. (2002) and creates the fundamental need for spatially continuous broadscale information to better understand and conserve freshwater fishes. Spatial

rich2/cjf-cjfas/cjf-cjfas/cjf99914/cjf0845d14z | xppws | S=3 | 12/16/16 | 7:26 | 4/Color Fig: F1,F4 | Art: **cjfas-2016-0247** | Input-1st disk, 2nd ??

Pagination not final (cite DOI) / Pagination provisoire (citer le DOI)

2

Can. J. Fish. Aquat. Sci. Vol. 00, 0000

sampling strategies like that espoused by Hankin and Reeves (1988) or more recent attempts (Stevens and Olsen 2004; Torgersen et al. 2006; Korman et al. 2016) partially address information needs but are costly and difficult to implement in hundreds of streams throughout the ranges of species or across the 100s–10 000s of linear kilometres that constitute river networks. Another critical and largely unrecognized impediment to developing spatial fisheries information has been the lack of consistent geospatial database frameworks for streams to enable efficient organization, summarization, and sharing of data within or among agencies (Cooter et al. 2010). Such frameworks would provide a database structure wherein each stream reach within a river network is assigned a unique identifier, attributed with topological information (e.g., up- and downstream flow-routing), and georeferenced in a cartographic projection system. Networks with those properties could bridge between relational databases (e.g., Access or Oracle) that are used to store large fisheries data sets and geographic information systems (GIS) that would be used to manipulate and visualize data associated with broadscale population estimation. Also required are flexible analytical tools for data collected from stream networks, especially those capable of accommodating the clustered, nonindependent sample locations that inevitably arise during the history of resource agencies or when data are aggregated from multiple sources.

In recent years, key statistical and technical advances addressed many of the preceding issues to provide the basic elements for creating a broadly scalable approach to population estimation. The development of spatial-stream-network (SSN) models (Ver Hoef et al. 2006; Ver Hoef and Peterson 2010) based on covariance structures for network topology (Peterson and Ver Hoef 2010) and that rely on assumptions about the stochastic processes generating observable data (Schabenberger and Gotway 2005) facilitates valid inference from nonindependent stream samples. As extensions of the linear-mixed model, SSNs accommodate covariates to describe relationships with response variables, and simulation studies indicate their accuracy in fixed effect parameter estimation and confidence interval coverage for a wide range of conditions (Som et al. 2014; Rushworth et al. 2015). Concerns have been raised about "spatial confounding" in the estimation of fixed effect parameters (Hodges and Reich 2015; but see Hanks et al. 2015 for a counter-argument), but such confounding is of limited relevance for making accurate spatial predictions. Like other spatial statistical models (Ver Hoef 2002; Beale et al. 2010; Temesgen and Ver Hoef 2015), SSNs consistently improve predictive performance relative to nonspatial models when used with spatially dense data sets that contain nonindependent samples (Isaak et al. 2010; Brennan et al. 2016; Turschwell et al. 2016). Classical geostatistical techniques (Cressie 1993) have also been adapted for implementation with the SSN models based on stream distances rather than Euclidean distances, which enables kriging and block-kriging (BK) predictions to be made throughout river networks with spatially explicit errors (Ver Hoef et al. 2006).

Paralleling the development of SSN models has been the development of nationally consistent geospatial frameworks for stream data (Cooter et al. 2010; Moore and Dewald 2016). Most notably for Canada, lotic systems are represented by the National Hydro Network (NHN; http://ftp2.cits.rncan.gc.ca/pub/geobase/official/nhn_rhn/doc/NHN.pdf) and within the United States by the National Hydrography Dataset (NHD; www.horizon-systems.com/NHDPlus/NHDPlusV2_home.php). The NHD is available in several resolutions, but of particular value is the medium resolution version (1:100 000 scale) because of the reach descriptor variables (e.g., elevation, slope, watershed size, and many others) that have been incorporated as value-added attributes to create NHDPlus

(McKay et al. 2012). The reach descriptors can be used to query stream networks, visualize results within a GIS, and as covariates in predictive models. As the user community associated with NHDPlus has grown, dozens of additional reach descriptors have been developed by groups like the National Fish Habitat Partnership (Wang et al. 2011) and the Environmental Protection Agency (Hill et al. 2016).

In this paper, we integrate SSN models and the geospatial resources described above with a fish density data set to develop a scalable approach to population estimation. Models that predict fish density are developed based on different combinations of covariates and autocovariance functions that account for nonindependence among samples. The models are used to predict continuous density maps, which are then summarized to make population estimates at stream, river, and network scales. For comparison with nonspatial analogues, estimates are also made using multiple linear regression (MLR) and simple random sampling (SRS). The data set and statistical code used in the analysis are included as online supplemental materials[1], so that interested readers may explore these topics in detail. **Fn1**

Materials and methods

Study area and data set

A data set of density estimates for different trout species at 108 sites was obtained from the 2300 km^2 Salt River watershed on the border between Idaho and Wyoming in the western US. The area is mountainous and 11 major tributaries drain north–south trending ranges at the eastern and western extents of the watershed (Fig. 1). Tributaries and several spring streams that originate from **F1** the main valley floor were sampled at 104 locations during summer low-flow conditions (stream widths: 1.2–8.8 m, reach lengths: 63–465 m) in 1996 and 1997 by electrofishing within block-netted reaches to obtain local population estimates for age-1+ trout using depletion methods (Zippin 1958; Isaak and Hubert 2004). Samples were spaced at 50 m elevation intervals along most tributaries, with additional samples taken near tributary confluences or upstream and downstream of abrupt contrasts in channel slope. Those data were supplemented with population estimates from four sites on the Salt River main stem (river widths: 20–32 m, reach lengths: 4.4–4.8 km) that were repeated in 1995, 1996, and 1998 by raft electrofishing using mark–recapture methods (Pollock et al. 1990; Gelwicks et al. 2002). For current purposes, the Salt River estimates were averaged across years. Species composition, based on approximately 5000 trout captured at the 108 sites, was 82.6% native Yellowstone cutthroat trout (*Oncorhynchus clarkii bouvieri*), 12.7% non-native brown trout (*Salmo trutta*), 4.6% non-native brook trout (*Salvelinus fontinalis*), and 0.1% non-native rainbow trout (*Oncorhynchus mykiss*). Population estimates at the 108 sites were standardized as trout·100 m^{-1} length of stream. Additional details about the data set and study area are provided elsewhere (Gelwicks et al. 2002; Isaak and Hubert 2004).

A digital stream network for the NHD processing unit (Pacific Northwest 17) that encompassed the Salt River watershed was downloaded from the National Stream Internet website (NSI; www.fs.fed.us/rm/boise/AWAE/projects/NationalStreamInternet.html; Isaak et al. 2013) and clipped using the watershed boundary. The NSI network is derived from the 1:100 000 scale NHDPlus version 2 network, has been topologically adjusted to facilitate SSN analysis using the Spatial Tools for the Analysis of River Systems software (STARS; Peterson and Ver Hoef 2014), and is available for all streams and rivers in the coterminous US. A one-to-one relationship between reaches in the NSI and NHDPlus networks facilitates the use of NHD reach descriptors as covariates in SSN models. Here, we considered only a small number of covariates (reach slope,

---

rich2/cjf-cjfas/cjf-cjfas/cjf99914/cjf0845d14z | xppws | S=3 | 12/16/16 | 7:26 | 4/Color Fig: F1,F4 | Art: **cjfas-2016-0247** | Input-1st disk, 2nd ??

Pagination not final (cite DOI) / Pagination provisoire (citer le DOI)

Fig. 1. Salt River watershed in the western US and locations of trout density estimates at 108 sites. Population estimates were subsequently made for areas upstream of the green bars on tributaries and downstream of the green bar on the Salt River mainstem. [Colour online.]
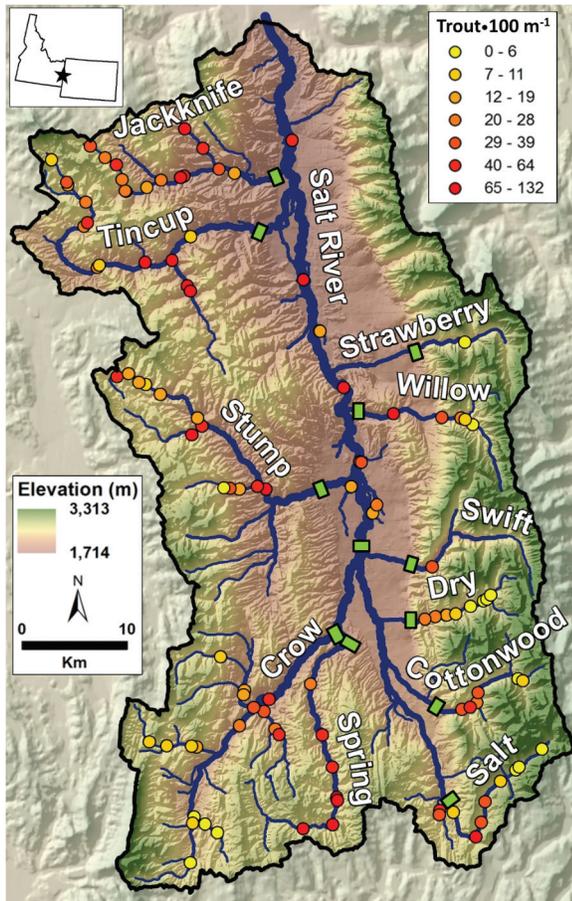
summer temperature, and stream canopy density), which have previously been associated with trout densities (Chisholm and Hubert 1986; Fausch et al. 1988; Isaak and Hubert 2004) and were available as reach descriptors in geospatial formats (Table 1). The NHD and NSI networks contain many reaches that do not support fish populations because of intermittent flow or excessive steepness, so the original Salt River network of 1901 km was trimmed to a 735 km network prior to analysis by deleting reaches with >10% slope, those coded as intermittent in the NHDPlus data set (e.g., Fcode = 46003), and based on observations made by the lead author during field sampling. We processed the final data set using the current version of STARS (Peterson and Ver Hoef 2014; version 2.0.4 downloaded from the SSN/STARS website: www.fs.fed.us/rm/boise/AWAE/projects/SpatialStreamNetworks.shtml) and output the spatial, topological, and attribute information as a Landscape Network object (LSN; available as Supplemental A[1]) suitable for spatial analysis. The SSN package (Ver Hoef et al. 2014; version 1.1.7) for the R statistical software (R Core Team 2014) was downloaded from the Comprehensive R Archive Network website (www.r-project.org/) and used with the LSN object to conduct all subsequent analyses.

To describe spatial similarity, often referred to as autocorrelation, in the trout density data set, a type of semivariogram called a Torgegram was initially calculated (Zimmerman and Ver Hoef 2017). The semivariance is one-half of the mean-squared difference between random variables separated by some intervening distance (Matheron 1963). If s_i and s_j contain the spatial coordinates for the ith and jth locations, and $y(s_i)$ and $y(s_j)$ are the mea-

sured values at those locations, then an empirical estimator of the semivariance, $\gamma(h)$, is

$$(1) \qquad \gamma(h) = \frac{1}{2N(h)} \sum_{\|s_i - s_j\| \in c(h)} [y(s_i) - y(s_j)]^2$$

where h is the distance, $\|s_i - s_j\|$, between locations, $c(h)$ is the distance bin representing the interval around h (chosen to be mutually exclusive and exhaustive so that all distances h fall into one of the bins), and $N(h)$ is the number of data pairs (s_i, s_j) in distance bin $c(h)$. The semivariogram provides a graphical representation of spatial autocorrelation in the measured data; when semivariance values are low (high), it indicates that sample pairs within a distance bin are similar (dissimilar). If positive autocorrelation occurs within a data set, the semivariance values are smallest at short distance lags and increase as distance increases. The Torgegram is similar to a traditional semivariogram except that semivariance values are plotted separately for site pairs with flow-connected (e.g., water flows from an upstream site through a downstream site) and flow-unconnected (e.g., sites reside on the same network but do not share the same flow) relationships, because these patterns usually differ on stream networks (Peterson et al. 2013; Zimmerman and Ver Hoef 2017). As expected, given the density of the trout samples, the Torgegram showed strong similarities among site estimates in close proximity and weaker similarities as separation distances increased (Fig. 2). Semivariance among flow-unconnected sites plateaued at approximately 10 km, while semivariance among flow-connected sites steadily increased to the maximum distance of 50 km. Those patterns indicated that trout densities became dissimilar among adjacent headwater streams (i.e., flow-unconnected relationships) over shorter geographic distances than did densities along flow-connected pathways from headwaters to the river mainstem.

SSN trout density models

Five SSN models were fit to the trout density data set in R using the SSN package (a copy of the R script is provided as Supplemental B[1]). Three of those models included reach covariates, and two models used only an intercept (i.e., mean trout density) with an autocovariance function (Table 2), which was equivalent to ordinary kriging. In all cases, the basic linear mixed model we used was

$$(2) \qquad \boldsymbol{y} = \mathbf{X}\boldsymbol{\beta} + \boldsymbol{z}_{\text{TU}} + \boldsymbol{z}_{\text{TD}} + \boldsymbol{z}_{\text{EUC}} + \boldsymbol{\varepsilon}$$

where $\boldsymbol{y}$ is a vector of measured trout densities, $\mathbf{X}$ is a matrix of covariate values, $\boldsymbol{\beta}$ is a vector of regression coefficients, and $\boldsymbol{\varepsilon}$ is a vector of independent and normally distributed random errors. The spatial structure in residuals was described using vectors of zero-mean random variables ($\boldsymbol{z}_{\text{TU}}$, $\boldsymbol{z}_{\text{TD}}$, and $\boldsymbol{z}_{\text{EUC}}$) with a autocorrelation structure based on tail-up (TU), tail-down (TD), and Euclidean (EUC) covariance functions (Peterson and Ver Hoef 2010, Ver Hoef and Peterson 2010). Each random variable ($\boldsymbol{z}_{\text{TU}}$, $\boldsymbol{z}_{\text{TD}}$, $\boldsymbol{z}_{\text{EUC}}$) in the autocorrelation structure can be represented by one of several different covariance models (e.g., linear-with-sill, Mariah, exponential, Epanechnikov, spherical models; Chiles and Delfiner 2009; Garreta et al. 2010). Moreover, one or more classes of covariance function (TU, TD, EUC) may be chosen to represent the properties of the stream attribute being modeled (e.g., patterns created by passive downstream diffusion or upstream and downstream movement processes). The choice of covariance function(s) is important because each represents spatial relationships in a different way. The TU function restricts correlation to sites that are flow-connected and uses spatial weighting based on user-specified stream attributes (e.g., watershed area, stream order, segment slope) to up- or down-weighted samples that occur up-

| rich2/cjf-cjfas/cjf-cjfas/cjf99914/cjf0845d14z | xppws | S=3 | 12/16/16 | 7:26 | 4/Color Fig: F1,F4 | Art: **cjfas-2016-0247** | Input-1st disk, 2nd ?? |

Pagination not final (cite DOI) / Pagination provisoire (citer le DOI)

4

Can. J. Fish. Aquat. Sci. Vol. 00, 0000

Table 1. Summary statistics for trout densities and geospatial representations of habitat characteristics at 108 reaches across the Salt River network.

Variable	Mean	Median	SD	Minimum	Maximum	Data source
Trout·100 m^{-1}	32.6	25.0	29.4	0	132	Gelwicks et al. 2002; Isaak and Hubert 2004
August mean stream temperature (°C)	11.1	11.5	2.42	5.06	15.6	NorWeST (www.fs.fed.us/rm/boise/AWAE/projects/NorWeST.html; Isaak et al. 2016)
Reach slope (%)	3.00	2.70	2.60	0.015	10.0	NHDPlus value-added attribute (www.horizon-systems.com/NHDPlus/index.php; McKay et al. 2012)
Canopy (%)	30.7	31.9	16.9	0	80.1	National Land Cover Dataset (www.mrlc.gov/nlcd2001.php; Homer et al. 2015)

Fig. 2. Empirical Torgegram describing patterns in spatial similarity among trout densities at 108 sites. Symbol sizes are proportional to the number of data pairs averaged for each semivariance value.
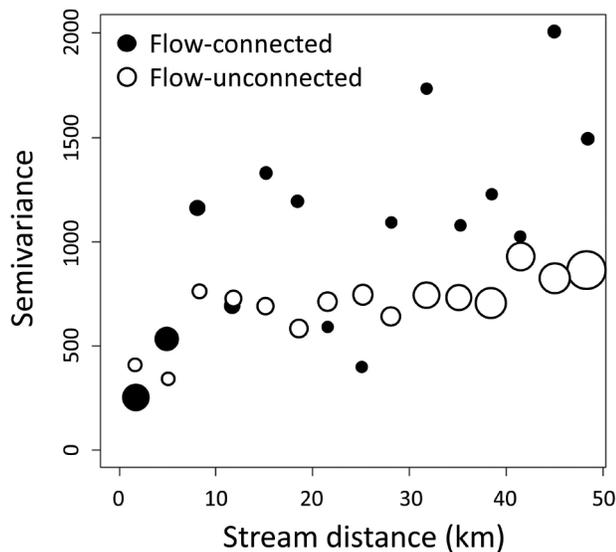
stream of a location (Frieden et al. 2014). The TD function, in contrast, permits correlation between both flow-connected and flow-unconnected locations and a spatial weighting scheme is not necessary. For simplicity, we drew on previous results that suggest a mixed covariance construction usually performs best (Peterson and Ver Hoef 2010; Frieden et al. 2014) and used exponential models for the TD, EUC, and TU functions, with the TU weighting scheme based on watershed area.

The five SSN models were compared using the Akaike information criterion (AIC; Akaike 1974), penalizing for the number of covariate and autocovariance parameters. Leave-one-out cross-validation (LOOCV) was used to assess the predictive performance of models in two ways. We computed r^2 for a linear model that related LOOCV predictions to observed trout densities, and we computed the root mean square prediction error as

$$(3) \qquad \text{RMSPE} = \sqrt{\frac{\sum_{i=1}^{n} [\hat{y}(s_i) - y(s_i)]^2}{n}}$$

where $y(s_i)$ is the observation at location s_i, $\hat{y}(s_i)$ is the LOOCV prediction value for s_i, and n is the total number of observed data values. Maximum likelihood (ML) estimation was used for parameter estimation so that AIC values were valid for model comparisons, but restricted maximum likelihood (REML) was used for all other estimation purposes (Ver Hoef et al. 2014). As a baseline for comparison with the SSN models, we also fit a nonspatial MLR model to the trout density data set, which was based on the assumption that residual errors were spatially independent. The

same set of performance metrics was also calculated for the MLR model.

BK population estimates

The SSN models were used to predict trout densities at 100 m intervals throughout the Salt River network using universal kriging (Cressie 1993). The kriging equations have two parts, predictions based on the linear regression model and adjustments based on local spatial autocorrelation:

$$(4) \qquad \hat{y}(s_0) = \mathbf{x}(s_0)'\hat{\boldsymbol{\beta}} + \mathbf{c}(s_0)'\boldsymbol{\Sigma}^{-1}(\mathbf{y} - \mathbf{X}\hat{\boldsymbol{\beta}})$$

where $\mathbf{x}(s_0)$ is a vector containing the covariate values at prediction location s_0, and the vector $\hat{\boldsymbol{\beta}}$ contains the estimated regression coefficients using REML, so $\mathbf{x}(s_0)'\hat{\boldsymbol{\beta}}$ forms the linear regression prediction. The remaining portion of eq. 4 is an adjustment for spatial autocorrelation, where $\mathbf{c}(s_0)$ is a vector of covariances among observed data and the prediction site, and $\boldsymbol{\Sigma}$ is the covariance matrix among observed data. This kriging formulation provides exact interpolations that "honor the data" in contrast with alternatives based on splines (Schabenberger and Gotway 2005). Local prediction variances (Ver Hoef 2008) are given by

$$(5) \qquad \widehat{\text{var}}[\hat{y}(s_0)] = \sigma_0^2 - \mathbf{c}(s_0)'\boldsymbol{\Sigma}^{-1}\mathbf{c}(s_0) + \mathbf{d}'(\mathbf{X}'\boldsymbol{\Sigma}^{-1}\mathbf{X})^{-1}\mathbf{d}$$

where $\sigma_0^2 = \text{var}[y(s_0)]$ (including all of the variance components) and $\mathbf{d} = \mathbf{x}(s_0)' - \mathbf{X}'\boldsymbol{\Sigma}^{-1}\mathbf{c}(s_0)$.

Population estimates were developed from the network predictions using BK, which predicts a mean value from an integral of a random surface. The mean integral for a portion of a stream network, B_0, is

$$(6) \qquad \hat{y}(B_0) = \frac{1}{b-a} \int_a^b y(u)du$$

If the integral is over a stream network, then integrals are done piecewise for each stream segment, added together, and then divided by the total length of the integrated stream. In practice, the integral is approximated using a grid of evenly spaced prediction points along the network. BK predictions and variances require modification of eqs. 4 and 5, wherein $\mathbf{c}(s_0)$ is replaced by $\mathbf{c}(B_0)$ and all pairwise covariances are computed between the observed data and the points on the grid used to approximate an integral. Similar modifications are required for σ_0^2 in eq. 5, and covariates need to be integrated as well. The necessary two-dimensional formulas are given in Ver Hoef (2008), have been adapted for streams (Ver Hoef et al. 2006), and the functionality is included in the SSN package so that BK predictions and variances can be easily generated by users (Ver Hoef et al. 2014).

To approximate the integrals for population estimates in the Salt River network, we created a grid of points at 100 m intervals throughout the network. The BK estimate of trout density over any network subset then yielded an estimate of the mean trout

rich2/cjf-cjfas/cjf-cjfas/cjf99914/cjf0845d14z | xppws | S=3 | 12/16/16 | 7:26 | 4/Color Fig: F1,F4 | Art: **cjfas-2016-0247** | Input-1st disk, 2nd ??

Pagination not final (cite DOI) / Pagination provisoire (citer le DOI)

Table 2. Summary statistics for multiple linear regression (MLR) and spatial-stream-network (SSN) models fit to trout density data at 108 sites in the Salt River network.

Model	Covariate	b (SE)	p value	Autocovariance*	n_p†	ΔAIC	CV $r^{2‡}$	RMSPE§
MLR	Intercept	−55.0 (20.5)	<0.01	—	4	27	0.19	26.3
	Slope	36.7 (126)	0.77					
	Temperature	6.75 (1.43)	<0.01					
	Canopy	0.379 (0.163)	0.02					
SSN1	Intercept	−51.6 (29.1)	0.08	TU, TD	9	1	0.49	21.0
	Slope	103 (103)	0.32					
	Temperature	6.61 (2.22)	<0.01					
	Canopy	0.255 (0.173)	0.14					
SSN2	Intercept	−51.4 (29.7)	0.09	TU, TD, EUC	11	5	0.49	20.9
	Slope	104 (104)	0.32					
	Temperature	6.60 (2.27)	<0.01					
	Canopy	0.249 (0.18)	0.16					
SSN3	Intercept	−18.3 (19.1)	0.34	TU, TD	7	0	0.49	20.8
	Temperature	4.57 (1.67)	<0.01					
SSN4	Intercept	31.9 (5.69)	<0.01	TU, TD	6	5	0.49	20.9
SSN5	Intercept	31.4 (9.00)	<0.01	TU, TD, EUC	8	7	0.50	20.5

*TU, tail-up; TD, tail-down; EUC, Euclidean.
†Number of model parameters. In addition to covariate parameters, SSN models include three to seven parameters associated with the autocovariance construction (Ver Hoef and Peterson 2010).
‡Squared correlation between the leave-one-out cross-validation prediction and observed trout densities.
§Root mean square prediction error.

Fig. 3. Comparison of leave-one-out cross-validation (LOOCV) predictions for trout density derived from a multiple linear regression (A) and a spatial-stream-network model (SSN3; B). Dashed lines indicate 1:1 relationship.


Results
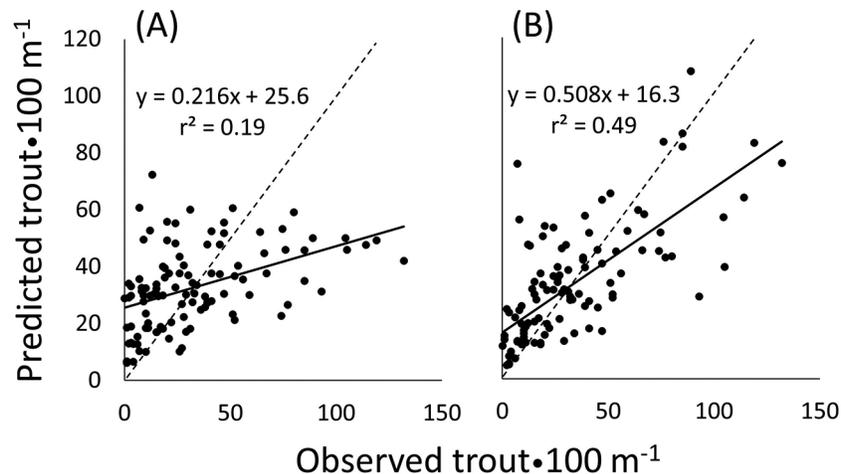
density, so the population estimate was this density times the length of the network subset. Figure 1 shows the locations where population estimates were made in tributaries and the Salt River main stem. The same BK procedure was conducted for the full network that supported fish populations to obtain a grand population estimate for the watershed. When making the grand estimate, we excluded downstream sections of some tributaries that are dewatered for irrigation purposes during the summer. As a baseline for comparison, we also derived population estimates for the same areas using a nonspatial SRS estimator with the observed densities (as in classical design-based surveys; Thompson 1992), which were then expanded based on appropriate stream-length factors.

Results

Trout densities at the 108 sites ranged from 0 to 132 trout·100 m^{-1} and showed geographic clustering of similar densities (Fig. 1) that corroborated the Torgegram results (Fig. 2). Densities were usually lowest in the highest elevation stream sites along the eastern portion of the watershed and higher in most western tributaries and the Salt River main stem. The five SSN models had similar

predictive accuracies (LOOCV $r^2 \sim 0.49$; RMSPE ~ 21.0) and showed considerable performance gains relative to the MLR (LOOCV $r^2 = 0.19$; RMSPE = 26.3; Table 2). Both types of models overestimated low densities and underestimated high densities, but the SSN models did so to a lesser degree (Fig. 3). The SSN models had AIC scores that were 20–27 points lower than the MLR, despite requiring the estimation of two to seven additional parameters for the autocovariance functions (Table 2). The temperature covariate was statistically significant in the models where it appeared ($p < 0.05$), and reach slope was never significant. The canopy covariate was significant in the MLR ($p = 0.02$) but not in the SSNs ($p \geq 0.14$). Within the SSN model set, SSN3 that used a temperature covariate and TU, TD autocovariance function had the lowest AIC value. Two models without covariates (SSN4 and SSN5) has similar predictive performance as SSN3 but had AIC scores 5–7 points higher. A trout density map predicted using SSN3 showed how abundance varied throughout the network (Fig. 4). Noteworthy was that predictions matched observed densities at the 108 sample sites, which is a property of the kriging formulation that was implemented. Also noteworthy was the spatial variation in the size of the prediction standard errors, which were smaller near sample

rich2/cjf-cjfas/cjf-cjfas/cjf99914/cjf0845d14z | xppws | S=3 | 12/16/16 | 7:26 | 4/Color Fig: F1,F4 | Art: **cjfas-2016-0247** | Input-1st disk, 2nd ??

Pagination not final (cite DOI) / Pagination provisoire (citer le DOI)

Fig. 4. Trout density map predicted by universal kriging and a spatial-stream-network model (SSN3) fit to 108 samples. Stream lines are colored by predicted values, and the width of the black stream border is proportional to prediction standard errors. Population estimates were made for areas upstream of the green bars on tributaries and downstream of the green bar on the Salt River main stem. Predictions were not made in the downstream extents of several eastern tributaries and an upper section of the Salt River where channels are dewatered during the summer. [Colour online.]
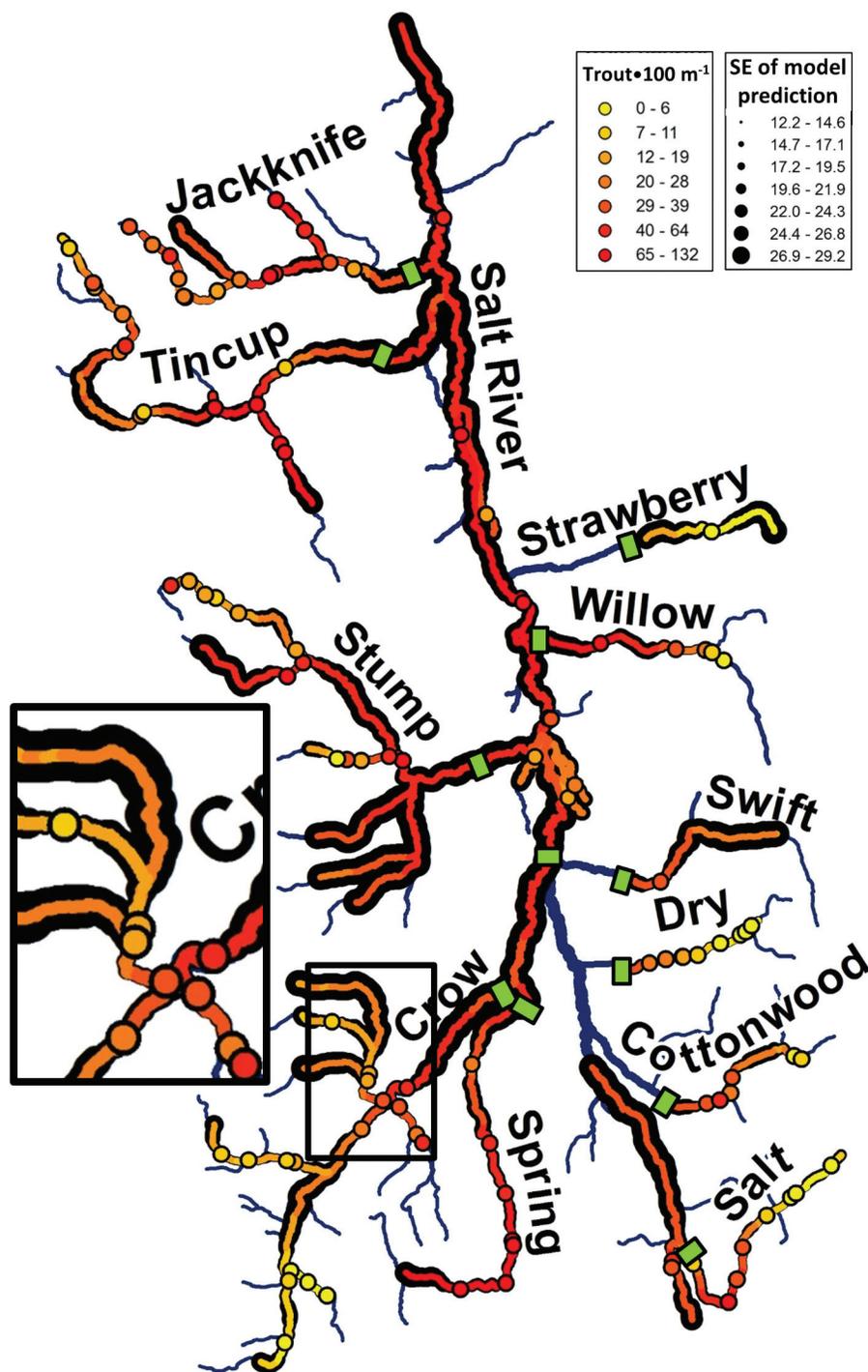
sites because the SSN model used the fitted autocovariance function and local empirical support when making predictions.

Population estimates based on SRS and the five SSN models showed several interesting properties when examined for four representative tributaries (Fig. 5). First, SSN–BK estimates could be made for all streams, which was not the case with the SRS estimator in Swift Creek where only one density sample was available

(two samples are needed to calculate a variance and confidence interval). Second, results from Willow Creek support the notion that SSN–BK estimates may often be more accurate than those from SRS. Five density samples were available in that stream, but only one occurred in the downstream segment where trout densities were high, so the SRS population estimate of ~4000 trout was biased low compared with the BK estimate of ~7000 trout

rich2/cjf-cjfas/cjf-cjfas/cjf99914/cjf0845d14z | xppws | S=3 | 12/16/16 | 7:26 | 4/Color Fig: F1,F4 | Art: **cjfas-2016-0247** | Input-1st disk, 2nd ??

Pagination not final (cite DOI) / Pagination provisoire (citer le DOI)

Fig. 5. Trout population estimates for four tributary streams derived from simple random sample (SRS) and spatial-stream-network (SSN) block-kriging estimators. Error bars denote 95% confidence intervals; sample sizes are the number of fish density surveys conducted within each tributary. An SRS estimate was not possible for Swift Creek, where a single site was sampled.
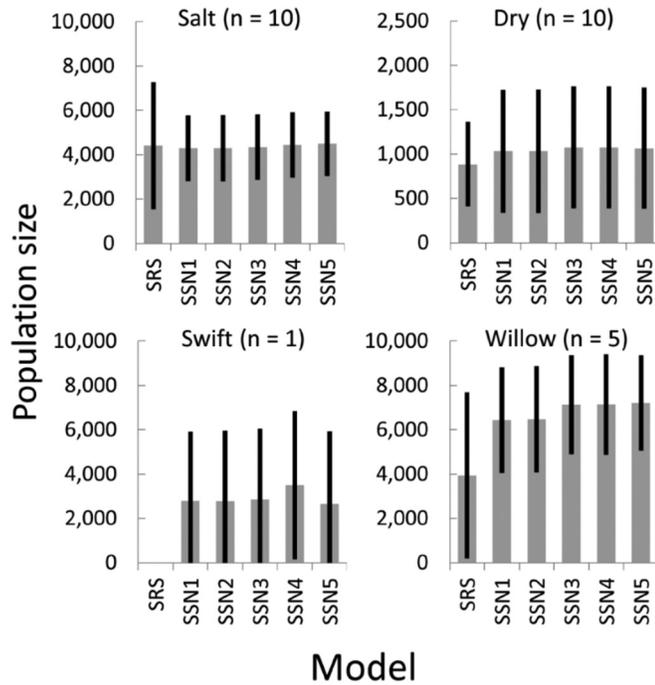
Fig. 6. Trout population estimates from simple random sample (SRS) and spatial-stream-network (SSN3) block-kriging estimators for the Salt River main stem and tributary streams draining the western (A) and eastern (B) sides of the watershed. Error bars denote 95% confidence intervals; SRS estimates were not possible for Strawberry Creek and Swift Creek, where single sites were sampled.
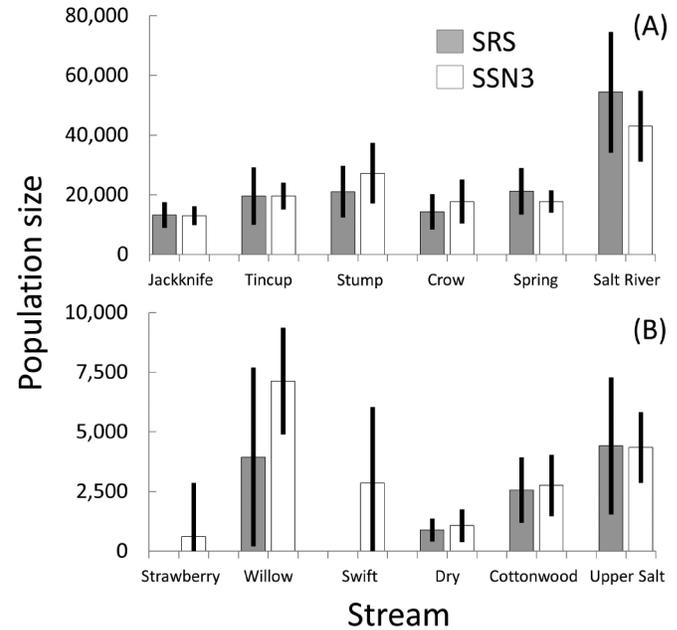
made from a spatially balanced set of predictions throughout the stream. Third, SSN–BK estimates for individual streams were similar regardless of the model chosen, which suggested robustness to different specifications.

A full set of SRS and SSN3–BK population estimates for streams in the Salt River network is provided in Fig. 6. The SSN3–BK estimates were usually more precise and showed that eastern tributaries had smaller trout populations (612–7128 trout) than western tributaries (12 963–27 216 trout) and the Salt River main stem (42 987 ± 11 894 trout (95% CI)). The difference in population estimates was primarily due to the shorter networks that comprised eastern tributaries, but those streams were also especially cold and may have been too unproductive to support high trout densities as indicated by the positive effect of the temperature covariate in the SSN models. The grand SSN3–BK population estimate for the Salt River network was 184 030 ± 27 263 trout, whereas the SRS estimate was 155 828 ± 26 514 trout. Similar to the bias associated with the Willow Creek estimate, the SRS estimate for the full network may have been biased by the large proportion of samples from high-elevation tributaries where trout densities were lower (Fig. 1). That bias could have been addressed using a stratified random sampling estimator wherein each tributary was treated as a stratum, but single samples from some strata would have made variance calculations impossible without ad hoc combinations of multiple streams into workable strata.

Discussion

Combining fish density surveys and SSN models with broadly available geospatial data frameworks creates a powerful and flexible approach to population estimation for streams and rivers. As we demonstrate, population estimates can be derived at virtually any spatial scale, thereby allowing biological information to be matched with relevant land uses, landscape features, or jurisdictional and biogeographic boundaries to address conservation and

management needs. For example, population estimates at stream or network scales are key for species' conservation assessments (e.g., the 50/500 rule; Franklin 1980), but have rarely been available or are based on extrapolations from a small number of non-random samples (Hilderbrand and Kershner 2000; Cook et al. 2010). Estimates like those developed here for the Salt River basin, which hosted ~150 000 of the native Yellowstone cutthroat trout (a species of conservation concern), can now be repeated elsewhere to inform status assessments where sufficient data exist. Although 50–100 samples are desirable to estimate parameters for the SSN models (Isaak et al. 2014), data sets of this size are common within research and management agencies, especially when data are aggregated across multiple projects or agencies. One example, the MARIS database (Multistate Aquatic Resources Information System: www.marisdata.org; Loftus and Beard 2009), contains >1 000 000 fisheries surveys for >1000 species in the eastern US, an impressive total that nonetheless represents a small fraction of extant data. Another potential application of the SSN–BK estimator was presented by the dewatered stream reaches in the Salt River network, where estimates could have been made for the number of trout those areas would support if perennial flows were restored. BK also has obvious utility for making reference site comparisons used in biological and habitat condition assessments (Kershner and Roper 2010; Hawkins et al. 2010) or within the regulatory arena to determine where standards are exceeded if SSN models are applied to water chemistry attributes (Birkeland 2001).

A key difference between SSN-BK and previous estimators (e.g., Hankin and Reeves 1988; Stevens and Olsen 2004) is that the SSN estimator relies on model-based inference and does not require random sampling (Ver Hoef 2008). Even when designs are randomized, better estimates are often possible using spatial models because random designs have some degree of clustering, and ancillary spatial information exists that is useful for estimation (Ver Hoef 2002). The SRS and MLR estimators used in our examples were unweighted, so clustered trout density samples over-represented

| rich2/cjf-cjfas/cjf-cjfas/cjf99914/cjf0845d14z | xppws | S=3 | 12/16/16 | 7:26 | 4/Color Fig: F1,F4 | Art: **cjfas-2016-0247** | Input-1st disk, 2nd ?? |

Pagination not final (cite DOI) / Pagination provisoire (citer le DOI)

8

Can. J. Fish. Aquat. Sci. Vol. 00, 0000

conditions in some areas and biased results because of spatial unbalance. Although it would have been possible to weight samples in an ad hoc fashion, BK finds an optimal weighting scheme within the blocking area. The SSN–BK estimator is accurate, therefore, because it replaces the mean of the observations with a mean from an evenly spaced grid of model predictions that achieves spatial balance. Each prediction is simply a weighted mean that has optimality properties, in the sense that it minimizes the mean-squared prediction error (Ver Hoef 2008).

Another important feature of the SSN models is their ability to incorporate covariates and assess effect sizes and statistical significance in the presence of spatial autocorrelation. Although the inclusion of covariates in our Salt River data set provided only small model improvements, developing fully descriptive density models here was not our goal. Those models are a logical next step, however, and one that will be enhanced by the availability of dozens of reach descriptors for the NHD and NSI networks (Wang et al. 2011; Hill et al. 2016) and the increasing technical proficiency of users in developing custom covariates (Peterson et al. 2011; Nagel et al. 2014). But as our results also demonstrate, informative covariates are not prerequisite to developing accurate prediction maps with SSN models if data sets are spatially dense and samples are autocorrelated. Those maps can provide detailed information about patterns of abundance and help identify fish density hotspots, which could be useful for directing conservation efforts even without a complete understanding of the processes that create spatial patterns. In the Salt River watershed, for example, the data visualization provided by the prediction maps added considerable depth to our view of the landscape despite a previous familiarity with it. Moreover, the depiction of spatial variation in SSN model prediction precision could be used to guide subsequent sampling efforts to locations that reduced the greatest amount of uncertainty. The Torgegram description of spatial autocorrelation among trout densities might also be useful for designing sampling campaigns in other networks that lack data by providing a first approximation of the stream distances over which samples are partially redundant (Som et al. 2014; Zimmerman and Ver Hoef 2017).

There are three caveats regarding the use of the SSN–BK estimator. First, population estimates for headwater streams will be sensitive to errors associated with the length of stream estimated to support fish, which may be problematic in that headwater reaches are often imprecisely mapped (Bishop et al. 2008). Our familiarity with the Salt River study site allowed us to trim the network based on field observations so that it closely approximated fish habitat, but the size of this reduction was substantial (61%) and would have inflated population estimates if not addressed. For applications where investigators lack direct knowledge of local conditions, rulesets to trim the network based on defensible criteria should be developed and applied. Two obvious criteria when using the NHDPlus data set are intermittency and stream slope. In the latter case, fish densities are low in steep reaches (Chisholm and Hubert 1986; Isaak et al. 2017), so exclusion of these areas in mountain landscapes has minor effects on population estimates. In arid landscapes like much of the American West, the network extent shown by NHDPlus is often far more extensive than the actual length of perennial streams, let alone those large enough to support fish populations (Fritz et al. 2013). Intermittent reaches are coded in NHDPlus (McKay et al. 2012), albeit inconsistently in different river basins, so may sometimes be identified and excluded from analysis. A second caveat pertains to preferential sampling and the possibility that strongly clustered sample locations could bias SSN model estimates (Diggle et al. 2010). Simulation results suggest SSN models perform well with many nonrandom samples (Falk et al. 2014; Som et al. 2014; Rushworth et al. 2015), but practitioners should always be cautious with ad hoc databases and avoid situations where models are fit to geographically restricted data and then extrapolated across

a much larger network extent. In addition to clustered samples, it is desirable to have some sample sites spread throughout the network to encompass a broad range of environmental conditions and ensure that parameter estimates and kriging predictions are robust (Courbois et al. 2008; Elith and Leathwick 2009). The third caveat associated with the SSN–BK estimator is that any systematic bias in local population estimates will translate to broadscale estimates, and the depletion estimator commonly used in small streams is negatively biased (Cook et al. 2010; Meyer and High 2011). That bias could be remedied by using mark–recapture techniques, conducting more electrofishing passes, incorporating detection efficiencies, or applying post hoc corrections (Peterson et al. 2004; Cook et al. 2010). Accurate local density estimates are desirable but increasing accuracy also comes at a cost when it requires longer sampling durations at individual sites (e.g., mark–recapture estimates). However, if the greatest uncertainty in a broadscale population estimate stems from sampling a small proportion of the total area, then sampling more sites less accurately could be optimal. That is especially true if the decrease in local accuracy is small, as is often the case with removal estimators because the number of fish captured during the first pass correlates strongly with final estimates based on multiple passes (Cook et al. 2010; Meyer and High 2011). Similar trade-offs are what ultimately motivated the systematic, broadscale sampling approach of Hankin and Reeves (1988), and a re-examination of this issue using the spatial statistical simulation capabilities provided in SSN software would be timely (Ver Hoef et al. 2014).

SSN models are powerful tools for stream scientists but the recency of their development also means that work remains to develop additional statistical theory and software that broadens their application. Most relevant to abundance estimation would be SSN models that incorporate habitat-related detection efficiencies (Peterson et al. 2004). However, application of those models, or any others, to large data sets aggregated from many sources face challenges associated with inconsistent field habitat measurement protocols (Millar et al. 2016). Standardization of protocols is needed but geospatial representations of habitat conditions that affect detection efficiency (e.g., stream size, reach slope, habitat complexity) may also be an effective alternative that could be implemented consistently across large areas as stream covariate databases and remote sensing applications continue to grow (Carbonneau et al. 2012; Hill et al. 2016). Space–time models are another logical extension of SSN models because repeat sampling of sites is fundamental to many fisheries monitoring programs (Thorson et al. 2015). Geostatistical space–time models have been developed for non-network systems (Cressie and Wikle 2011), but their adaption to streams with appropriate covariance structures is a nontrivial task that requires additional research.

We are not the first to recognize the potential benefits of geostatistical methods for stream and river data (Ganio et al. 2005; Durance et al. 2006), nor is this the first attempt to use geospatial technologies to derive population estimates at broader scales (Wyatt 2003; Webster et al. 2008). Only recently, however, has the statistical theory for stream networks developed sufficiently (Peterson et al. 2010; Ver Hoef et al. 2010) and been integrated into robust software (Peterson and Ver Hoef 2014; Ver Hoef et al. 2014) to make the methods broadly accessible to users. The timing is opportune given the increasing availability of large, spatially dense fisheries data sets and geospatial frameworks for organizing data (Cooter et al. 2010; McKay et al. 2012). Developing initial SSN-BK population estimates may require a few weeks of work by those with complementary GIS and statistical skills, but it then is possible to derive population estimates at any scale within the modeling domain and to later refine population estimates with additional data. The insights yielded by these new spatial analyses regarding the distribution and abundance of stream fishes should prove useful in addressing many conservation and management issues.

Pagination not final (cite DOI) / Pagination provisoire (citer le DOI)

References

Akaike, H. 1974. A new look at the statistical model identification. IEEE Trans Automat Control, **19**(6): 716–722. doi:10.1109/TAC.1974.1100705.

Al-Chokhachy, R., Budy, P., and Schaller, H. 2005. Understanding the significance of redd counts: a comparison between two methods for estimating the abundance of and monitoring bull trout populations. N. Am. J. Fish. Manage. **25**(4): 1505–1512. doi:10.1577/M05-006.1.

Beale, C.M., Lennon, J.J., Yearsley, J.M., Brewer, M.J., and Elston, D.A. 2010. Regression analysis of spatial data. Ecol. Lett. **13**(2): 246–264. doi:10.1111/j.1461-0248.2009.01422.x. PMID:20102373.

Birkeland, S. 2001. EPA's TMDL program. Ecol. Law Q. **28**(2): 297–325. doi:10.15779/Z38F85M.

Bishop, K., Buffam, I., Erlandsson, M., Fölster, J., Laudon, H., Seibert, J., and Temnerud, J. 2008. *Aqua Incognita*: the unknown headwaters. Hydrol. Proc. **22**(8): 1239–1242. doi:10.1002/hyp.7049.

Brennan, S.R., Torgersen, C.E., Hollenbeck, J.P., Fernandez, D.P., Jensen, C.K., and Schindler, D.E. 2016. Dendritic network models: improving isoscapes and quantifying influence of landscape and in-stream processes on strontium isotopes in rivers. Geophys. Res. Lett. **43**(10): 5043–5051. doi:10.1002/2016GL068904.

Carbonneau, P., Fonstad, M.A., Marcus, W.A., and Dugdale, S.J. 2012. Making riverscapes real. Geomorphology, **137**(1): 74–86. doi:10.1016/j.geomorph.2010.09.030.

Chiles, J.P., and Delfiner, P. 2009. Geostatistics: modeling spatial uncertainty. John Wiley and Sons.

Chisholm, I.M., and Hubert, W.A. 1986. Influence of stream gradient on standing stock of brook trout in the Snowy Range, Wyoming. Northw. Sci. **60**(2): 137–139.

Cook, N., Rahel, F.J., and Hubert, W.A. 2010. Persistence of Colorado River Cutthroat Trout populations in isolated headwater streams of Wyoming. Trans. Am. Fish. Soc. **139**(5): 1500–1510. doi:10.1577/T09-133.1.

Cooter, W., Rineer, J., and Bergenroth, B. 2010. A nationally consistent NHDPlus framework for identifying interstate waters: implications for integrated assessments and interjurisdictional TMDLs. Environ. Manage. **46**(3): 510–524. doi:10.1007/s00267-010-9526-y. PMID:20625899.

Courbois, J.-Y., Katz, S.L., Isaak, D.J., Steel, E.A., Thurow, R.F., Wargo Rub, A.M., Olsen, T., and Jordan, C.E. 2008. Evaluating probability sampling strategies for estimating redd counts: an example with Chinook salmon (*Oncorhynchus tshawytscha*). Can. J. Fish. Aquat. Sci. **65**(9): 1814–1830. doi:10.1139/F08-092.

Cressie, N. 1993. Statistics for spatial data. Revised ed. John Wiley and Sons, New York.

Cressie, N., and Wikle, C.K. 2011. Statistics for spatio-temporal data. John Wiley and Sons, Hoboken, New Jersey.

Diggle, P.J., Menezes, R., and Su, T.L. 2010. Geostatistical inference under preferential sampling. J. R. Stat. Soc. Ser. C Appl. Stat. **59**(2): 191–232. doi:10.1111/j.1467-9876.2009.00701.x.

Dunham, J.B., Rosenberger, A.E., Thurow, R.F., Dolloff, C.A., and Howell, P.J. 2009. Coldwater fish in wadeable streams. *In* Standard methods for sampling North American freshwater fishes. *Edited by* S.A. Bonar, W.A. Hubert, and D.W. Willis. American Fisheries Society, Bethesda, Md. pp. 119–138.

Durance, I., Le Pichon, C., and Ormerod, S.J. 2006. Recognizing the importance of scale in the ecology and management of riverine fish. River Res. Appl. **22**(10): 1143–1152. doi:10.1002/rra.965.

Elith, J., and Leathwick, J.R. 2009. Species distribution models: ecological explanation and prediction across space and time. Annu. Rev. Ecol. Evol. Syst. **40**(1): 677–697. doi:10.1146/annurev.ecolsys.110308.120159.

Falk, M.G., McGree, J.M., and Pettitt, A.N. 2014. Sampling designs on stream networks using the pseudo-Bayesian approach. Environ. Ecol. Stat. **21**(4): 751–773. doi:10.1007/s10651-014-0279-2.

Falke, J.A., Dunham, J.B., Jordan, C.E., McNyset, K.M., and Reeves, G.H. 2013. Spatial ecological processes and local factors predict the distribution and abundance of spawning by steelhead (*Oncorhynchus mykiss*) across a complex riverscape. PLoS ONE, **8**(11): e79232. doi:10.1371/journal.pone.0079232. PMID:24265762.

Fausch, K.D., Hawkes, C.L., and Parsons, M.G. 1988. Models that predict standing crop of stream fish from habitat variables: 1950–85. Gen. Tech. Rep. PNW-GTR-213. US Department of Agriculture, Forest Service, Pacific Northwest Research Station, Portland, Ore.

Fausch, K.D., Torgersen, C.E., Baxter, C.V., and Li, H.W. 2002. Landscapes to riverscapes: bridging the gap between research and conservation of stream fishes. BioScience, **52**(6): 483–498. doi:10.1641/0006-3568(2002)052[0483:LTRBTG]2.0.CO;2.

Franklin, I.R. 1980. Evolutionary change in small populations. *In* Conservation biology: an evolutionary–ecological perspective. *Edited by* M.E. Soulé and B.A. Wilcox. Sinauer, Sunderland, Mass. pp. 135–149.

Frieden, J.C., Peterson, E.E., Webb, J.A., and Negus, P.M. 2014. Improving the predictive power of spatial statistical models of stream macroinvertebrates using weighted autocovariance functions. Environ. Model. Softw. **60**: 320–330. doi:10.1016/j.envsoft.2014.06.019.

Fritz, K.M., Hagenbuch, E., D'Amico, E., Reif, M., Wigington, P.J., Jr., Leibowitz, S.G., Comeleo, R.L., Ebersole, J.L., and Nadeau, T. 2013. Comparing the extent and permanence of headwater streams from two field surveys to values from hydrographic databases and maps. J. Am. Water Resour. Assoc. **49**(4): 867–882. doi:10.1111/jawr.12040.

Ganio, L.M., Torgersen, C.E., and Gresswell, R.E. 2005. A geostatistical approach for describing spatial pattern in stream networks. Front. Ecol. Environ. **3**(3): 138–144. doi:10.1890/1540-9295(2005)003[0138:AGAFDS]2.0.CO;2.

Garreta, V., Monestiez, P., and Ver Hoef, J.M. 2010. Spatial modelling and prediction on river networks: up model, down model or hybrid? Environmetrics, **21**(5): 439–456. doi:10.1002/env.995.

Gelwicks, K.R., Zafft, D.J., and Gipson, R.G. 2002. Comprehensive study of the Salt River fishery between Afton and Palisades Reservoir from 1995 to 1999 with historical review: fur trade to 1998. Wyoming Game and Fish Department, Fish Division, Cheyenne.

Hankin, D.G., and Reeves, G.H. 1988. Estimating total fish abundance and total habitat area in small streams based on visual estimation methods. Can. J. Fish. Aquat. Sci. **45**(5): 834–844. doi:10.1139/f88-101.

Hanks, E.M., Schliep, E.M., Hooten, M.B., and Hoeting, J.A. 2015. Restricted spatial regression in practice: geostatistical models, confounding, and robustness under model misspecification. Environmetrics, **26**(4): 243–254. doi:10.1002/env.2331.

Hawkins, C.P., Olsen, J.R., and Hill, R.A. 2010. The reference condition: predicting benchmarks for ecological and water-quality assessments. J. N. Am. Benthol. Soc. **29**(1): 312–343. doi:10.1899/09-092.1.

Hilborn, R., and Walters, C.J. 1992. Quantitative fisheries stock assessment: choice, dynamics, and uncertainty. Chapman and Hall, New York.

Hilderbrand, R.H., and Kershner, J.L. 2000. Conserving inland cutthroat trout in small streams: how much stream is enough? N. Am. J. Fish. Manage. **20**(2): 513–520. doi:10.1577/1548-8675(2000)020<0513:CICTIS>2.3.CO;2.

Hill, R.A., Weber, M.H., Leibowitz, S.G., Olsen, A.R., and Thornbrugh, D.J. 2016. The stream-catchment (StreamCat) dataset: a database of watershed metrics for the conterminous United States. J. Am. Water Res. Assoc. **52**(1): 120–128. doi:10.1111/1752-1688.12372.

Hodges, J.S., and Reich, B.J. 2010. Adding spatially-correlated errors can mess up the fixed effect you love. Am. Stat. **64**(4): 325–334. doi:10.1198/tast.2010.10052.

Homer, C.G., Dewitz, J.A., Yang, L., Jin, S., Danielson, P., Xian, G., Coulston, J., Herold, N.D., Wickham, J.D., and Megown, K. 2015. Completion of the 2011 National Land Cover Database for the conterminous United States — Representing a decade of land cover change information. Photogramm. Eng. Remote Sens. **81**(5): 345–354.

Isaak, D.J., and Hubert, W.A. 2004. Nonlinear response of trout abundance to summer stream temperatures across a thermally diverse montane landscape. Trans. Am. Fish. Soc. **133**(5): 1254–1259. doi:10.1577/T03-010.1.

Isaak, D.J., Luce, C.H., Rieman, B.E., Nagel, D.E., Peterson, E.E., Horan, D.L., Parkes, S., and Chandler, G.L. 2010. Effects of climate change and wildfire on stream temperatures and salmonid thermal habitat in a mountain river network. Ecol. Appl. **20**(5): 1350–1371. doi:10.1890/09-0822.1. PMID:20666254.

Isaak, D.J., Peterson, E.E., Nagel, D.E., Ver Hoef, J.M., and Kershner, J. 2013. A national stream internet to facilitate accurate, high-resolution status and trend assessments for water quality parameters and aquatic biotas [online]. US Fish and Wildlife Service, National Landscape Conservation Cooperative grant. Available from www.fs.fed.us/rm/boise/AWAE/projects/NationalStreamInternet.html.

Isaak, D.J., Peterson, E.E., Ver Hoef, J.M., Wenger, S., Falke, J., Torgersen, C., Sowder, C., Steel, A., Fortin, M., Jordan, C., Reusch, A., Som, N., and Monestiez, P. 2014. Applications of spatial statistical network models to stream data. WIRES -Water, **1**(3): 277–294. doi:10.1002/wat2.1023.

Isaak, D.J., Wenger, S.J., Peterson, E.E., Ver Hoef, J.M., Hostetler, S., Luce, C.H., Dunham, J.B., Kershner, J., Roper, B.B., Nagel, D.E., Chandler, G.L., Wollrab, S., Parkes, S., and Horan, D.L. 2016. NorWeST modeled summer stream temperature scenarios for the western U.S. US Forest Service, Rocky Mountain Research Station Research Data Archive. doi:10.2737/RDS-2016-0033.

Isaak, D.J., Wenger, S., and Young, M.K. 2017. Big biology meets microclimatology: Defining thermal niches of aquatic ectotherms at landscape scales for conservation planning. Ecol. Appl. [In press.]

Kershner, J.L., and Roper, B.B. 2010. An evaluation of management objectives used to assess stream habitat conditions on federal lands within the interior Columbia Basin. Fisheries, **35**(6): 269–278. doi:10.1577/1548-8446-35.6.269.

Korman, J., Schick, J., and Mossop, B. 2016. Estimating riverwide abundance of juvenile fish populations: How much sampling is enough? N. Am. J. Fish. Manage. **36**(2): 213–229. doi:10.1080/02755947.2015.1114542.

Lincoln, F.C. 1930. Calculating waterfowl abundance on the basis of banding returns. United States Department of Agriculture Circular, Vol. 118. pp. 1–4.

rich2/cjf-cjfas/cjf-cjfas/cjf99914/cjf0845d14z | xppws | S=3 | 12/16/16 | 7:26 | 4/Color Fig: F1,F4 | Art: **cjfas-2016-0247** | Input-1st disk, 2nd ??

Pagination not final (cite DOI) / Pagination provisoire (citer le DOI)

10

Loftus, A.J., and Beard, T.D. 2009. The multistate aquatic resources information system (MARIS): Sharing data across agency boundaries. *In* Standard methods for sampling North American freshwater fishes. *Edited by* S.A. Bonar, W.A. Hubert, and D.W. Willis. American Fisheries Society, Bethesda, Md.

Matheron, G. 1963. Principles of geostatistics. Econ. Geol. **58**(8): 1246–1266. doi:10.2113/gsecongeo.58.8.1246.

McKay, L., Bondelid, T., Dewald, T., Johnston, J., Moore, R., and Rea, A. 2012. NHDPlus Version 2: user guide [online]. Available from ftp://ftp.horizon-systems.com/NHDPlus/NHDPlusV21/Documentation/NHDPlusV2_User_Guide.pdf.

Meyer, K.A., and High, B. 2011. Accuracy of removal electrofishing estimates of trout abundance in Rocky Mountain streams. N. Am. J. Fish. Manage. **31**(5): 923–933. doi:10.1080/02755947.2011.633684.

Meyer, K.A., Lamansky, J.A., Schill, D.J., and Zaroban, D.W. 2013. Nongame fish species distribution and habitat associations in the Snake River basin of southern Idaho. West. N. Am. Nat. **73**(1): 20–34. doi:10.3398/064.073.0102.

Millar, C.P., Fryer, R.J., Millidine, K.J., and Malcolm, I.A. 2016. Modelling capture probability of Atlantic salmon (*Salmo salar*) from a diverse national electrofishing dataset: Implications for the estimation of abundance. Fish. Res. **177**(1): 1–12. doi:10.1016/j.fishres.2016.01.001.

Moore, R.B., and Dewald, T.G. 2016. The road to NHDPlus — advancements in digital stream networks and associated catchments. J. Am. Water Resour. Assoc. doi:10.1111/1752-1688.12389.

Nagel, D.E., Buffington, J.M., Parkes, S.L., Wenger, S., and Goode, J.R. 2014. A landscape scale valley confinement algorithm: delineating unconfined valley bottoms for geomorphic, aquatic, and riparian applications. Gen. Tech. Rep. RMRS-GTR-321. US Department of Agriculture, Forest Service, Rocky Mountain Research Station Fort Collins, Colo.

Petersen, C.G. 1896. The yearly immigration of young plaice into the Limfjord from the German Sea. Report of the Danish Biological Station, Vol. 6. pp. 5–84.

Peterson, E.E., and Ver Hoef, J.M. 2010. A mixed-model moving-average approach to geostatistical modeling in stream networks. Ecology, **91**(3): 644–651. doi:10.1890/08-1668.1. PMID:20426324.

Peterson, E.E., and Ver Hoef, J.M. 2014. STARS: an ArcGIS toolset used to calculate the spatial information needed to fit spatial statistical models to stream network data. J. Stat. Softw. **56**(2): 1–17. doi:10.18637/jss.v056.i02.

Peterson, E.E., Sheldon, F., Darnell, R., Bunn, S.E., and Harch, B.D. 2011. A comparison of spatially explicit landscape representation methods and their relationship to stream condition. Freshw. Biol. **56**(3): 590–610. doi:10.1111/j.1365-2427.2010.02507.x.

Peterson, E.E., Ver Hoef, J.M., Isaak, D.J., Falke, J.A., Fortin, M.J., Jordan, C.E., McNyset, K., Monestiez, P., Ruesch, A.S., Sengupta, A., and Som, N. 2013. Modelling dendritic ecological networks in space: an integrated network perspective. Ecol. Lett. **16**(5): 707–719. doi:10.1111/ele.12084. PMID:23458322.

Peterson, J.T., Thurow, R.F., and Guzevich, J.W. 2004. An evaluation of multipass electrofishing for estimating the abundance of stream-dwelling salmonids. Trans. Am. Fish. Soc. **133**(2): 462–475. doi:10.1577/03-044.

Pollock, K.H., Nichols, J.D., Brownie, C., and Hines, J.E. 1990. Statistical inference for capture–recapture experiments. Wildlife Monographs, No. 107.

R Core Team. 2014. R: a language and environment for statistical computing. R Foundation for Statistical Computing, Vienna, Austria.

Rushworth, A.M., Peterson, E.E., Ver Hoef, J.M., and Bowman, A.W. 2015. Validation and comparison of geostatistical and spline models for spatial stream networks. Environmetrics, **26**(5): 327–338. doi:10.1002/env.2340. PMID:27563267.

Schabenberger, O., and Gotway, C.A. 2005. Statistical methods for spatial data analysis. Chapman and Hall/CRC, Boca Raton, Fla.

Schlosser, I.J. 1991. Stream fish ecology: a landscape perspective. BioScience, **41**(10): 704–712. doi:10.2307/1311765.

Som, N.A., Monestiez, P., Ver Hoef, J.M., Zimmerman, D.L., and Peterson, E.E. 2014. Spatial sampling on streams: principles for inference on aquatic networks. Environmetrics, **25**(5): 306–323. doi:10.1002/env.2284.

Stevens, D.L., Jr., and Olsen, A.R. 2004. Spatially balanced sampling of natural resources. J. Am. Stat. Assoc. **99**(465): 262–278. doi:10.1198/016214504000000250.

Temesgen, H., and Ver Hoef, J.M. 2015. Evaluation of the spatial linear model, random forest and gradient nearest-neighbor methods for imputing potential productivity and biomass of the Pacific Northwest forests. Forestry, **88**(1): 131–142. doi:10.1093/forestry/cpu036.

Thompson, S.K. 1992. Sampling. John Wiley & Sons, New York.

Thorson, J.T., Ianelli, J.N., Munch, S.B., Ono, K., and Spencer, P.D. 2015. Spatial delay-difference models for estimating spatiotemporal variation in juvenile production and population abundance. Can. J. Fish. Aquat. Sci. **72**(12): 1897–1915. doi:10.1139/cjfas-2014-0543.

Torgersen, C.E., Baxter, C.V., Li, H.W., and McIntosh, B.A. 2006. Landscape influences on longitudinal patterns of river fishes: spatially continuous analysis of fish–habitat relationships. *In* Landscape influences on stream habitats and biological assemblages. Vol. 48. *Edited by* R.M. Hughes, L. Wang, and P.W. Seelbach. American Fisheries Society, Bethesda, Md. pp. 473–492.

Turschwell, M.P., Peterson, E.E., Balcombe, S.R., and Sheldon, F. 2016. To aggregate or not? Capturing the spatio-temporal complexity of the thermal regime. Ecol. Indic. **67**: 39–48. doi:10.1016/j.ecolind.2016.02.014.

Ver Hoef, J.M. 2002. Sampling and geostatistics for spatial data. Ecoscience, **9**(2): 152–161. doi:10.1080/11956860.2002.11682701.

Ver Hoef, J.M. 2008. Spatial methods for plot-based sampling of wildlife populations. Environ. Ecol. Stat. **15**(1): 3–13. doi:10.1007/s10651-007-0035-y.

Ver Hoef, J.M., and Peterson, E.E. 2010. A moving average approach for spatial statistical models of stream networks. J. Am. Stat. Assoc. **105**(489): 6–18. doi:10.1198/jasa.2009.ap08248.

Ver Hoef, J.M., Peterson, E.E., and Theobald, D. 2006. Spatial statistical models that use flow and stream distance. Environ. Ecol. Stat. **13**(4): 449–464. doi:10.1007/s10651-006-0022-8.

Ver Hoef, J.M., Peterson, E.E., Clifford, D., and Shah, R. 2014. SSN: an R package for spatial statistical modeling on stream networks. J. Stat. Softw. **56**(3): 1–45. doi:10.18637/jss.v056.i03.

Wang, L., Infante, D., Esselman, P., Cooper, A., Wu, D., Taylor, W., Beard, D., Whelan, G., and Ostroff, A. 2011. A hierarchical spatial framework and database for the national river fish habitat condition assessment. Fisheries, **36**(9): 436–449. doi:10.1080/03632415.2011.607075.

Webster, R.A., Pollock, K.H., Ghosh, S.K., and Hankin, D.G. 2008. Bayesian spatial modeling of data from unit-count surveys of fish in streams. Trans. Am. Fish. Soc. **137**(2): 438–453. doi:10.1577/T06-138.1.

Wenger, S., Isaak, D.J., Luce, C., Neville, H., Fausch, K., Dunham, J., Dauwalter, D., Young, M., Elsner, M., Rieman, B., Hamlet, A., and Williams, J. 2011. Flow regime, temperature, and biotic interactions drive differential declines of Rocky Mountain trout species under climate change. Proc. Nat. Acad. Sci. **108**(34): 14175–14180. doi:10.1073/pnas.1103097108. PMID:21844354.

Wyatt, R.J. 2003. Mapping the abundance of riverine fish populations: integrating hierarchical Bayesian models with a geographic information system (GIS). Can. J. Fish. Aquat. Sci. **60**(8): 997–1006. doi:10.1139/f03-085.

Zale, A.V., Parrish, D.L., and Sutton, T.M. 2013. Fisheries techniques. 3rd ed. American Fisheries Society, Bethesda, Md.

Zimmerman, D., and Ver Hoef, J.M. 2017. The Torgegram for fluvial variography: characterizing spatial dependence on stream networks. J. Comp. Graph. Stat. doi:10.1080/10618600.2016.1247006.

Zippin, C. 1958. The removal method of population estimation. J. Wildl. Manage. **22**(1): 82–90. doi:10.2307/3797301.

Supplemental A.
A ZIP file containing the LSN object file "LSN_TroutDensity_BlockKrige.ssn" and ESRI geodatabase "LSN_TroutDensity_BlockKrige.mdb" to replicate the Salt River analysis is downloadable at the SSN/STARS website "Software and Data" subpage (www.fs.fed.us/rm/boise/AWAE/projects/SSN_STARS/software_data.html).

The annotated R script "SaltRiver_TroutDensity_BlockKriging.R" given below is used to model trout densities in the Salt River and derive block-kriging population estimates with the LSN object files above.

```
#Load SSN package into R
library("SSN")

#Set working directory to location of .ssn directory
setwd("C:\\...")

#import the data from the .ssn directory and create a SpatialStreamNetwork object with basic set of prediction
points for all reach midpoints
SaltWQ <- importSSN("lsndata/LSN_TroutDensity_BlockKrige.ssn", predpts = "preds")

#Import prediction points spaced at 100m intervals for block-kriging estimates of individual streams
SaltWQ <- importPredpts(SaltWQ, "Cottonwood", "ssn")
SaltWQ <- importPredpts(SaltWQ, "Crow", "ssn")
SaltWQ <- importPredpts(SaltWQ, "Dry", "ssn")
SaltWQ <- importPredpts(SaltWQ, "Jackknife", "ssn")
SaltWQ <- importPredpts(SaltWQ, "Salt", "ssn")
SaltWQ <- importPredpts(SaltWQ, "Spring", "ssn")
SaltWQ <- importPredpts(SaltWQ, "Strawberry", "ssn")
SaltWQ <- importPredpts(SaltWQ, "Stump", "ssn")
SaltWQ <- importPredpts(SaltWQ, "Swift", "ssn")
SaltWQ <- importPredpts(SaltWQ, "Tincup", "ssn")
SaltWQ <- importPredpts(SaltWQ, "Willow", "ssn")
SaltWQ <- importPredpts(SaltWQ, "SaltRiver", "ssn")

#Import prediction points spaced at 100m intervals for block-kriging estimate of full network
SaltWQ <- importPredpts(SaltWQ, "Network", "ssn")

#Create distance matrices among stream prediction points
createDistMat(SaltWQ, predpts = "preds", o.write = TRUE, amongpreds = TRUE)
createDistMat(SaltWQ, predpts = "Cottonwood", o.write = TRUE, amongpreds = TRUE)
createDistMat(SaltWQ, predpts = "Crow", o.write = TRUE, amongpreds = TRUE)
createDistMat(SaltWQ, predpts = "Dry", o.write = TRUE, amongpreds = TRUE)
createDistMat(SaltWQ, predpts = "Jackknife", o.write = TRUE, amongpreds = TRUE)
createDistMat(SaltWQ, predpts = "Salt", o.write = TRUE, amongpreds = TRUE)
createDistMat(SaltWQ, predpts = "Spring", o.write = TRUE, amongpreds = TRUE)
createDistMat(SaltWQ, predpts = "Strawberry", o.write = TRUE, amongpreds = TRUE)
createDistMat(SaltWQ, predpts = "Stump", o.write = TRUE, amongpreds = TRUE)
createDistMat(SaltWQ, predpts = "Swift", o.write = TRUE, amongpreds = TRUE)
createDistMat(SaltWQ, predpts = "Tincup", o.write = TRUE, amongpreds = TRUE)
createDistMat(SaltWQ, predpts = "Willow", o.write = TRUE, amongpreds = TRUE)
```

createDistMat(SaltWQ, predpts = "SaltRiver", o.write = TRUE, amongpreds = TRUE)

#Create distance matrix among network prediction points (calculations require a few minutes)
createDistMat(SaltWQ, predpts = "Network", o.write = TRUE, amongpreds = TRUE)

#Describe the names of the variables in the point.data data.frame for each observed and prediction data set
names(SaltWQ)

#plot Salt River network and locations of 108 trout density observations
plot(SaltWQ, lwdLineCol = "afvArea", lwdLineEx = 5, lineCol = "blue",
  pch = 19, xlab = "x-coordinate (m)", ylab = "y-coordinate (m)", asp = 1)

#plot values of 108 trout density observations (Figure 1)
brks <- plot(SaltWQ, "trout_100m", lwdLineCol = "afvArea",
  lwdLineEx = 5, lineCol = "black", xlab = "x-coordinate" ,
  ylab = "y-coordinate", asp=1)

#plot Torgegram based on 108 trout density observations (Figure 2)
SaltWQ.Torg <- Torgegram(SaltWQ, "trout_100m", nlag = 15, nlagcutoff = 1, maxlag = 50000)
plot(SaltWQ.Torg)

#Fit nonspatial multiple linear regression (MLR) in Table 2
SaltWQ.glmssn0 <- glmssn(trout_100m ~ SLOPE + S1_93_11 + CANOPY, SaltWQ,
  CorModels = NULL, use.nugget = TRUE, EstMeth = "REML")
summary(SaltWQ.glmssn0)

#Fit SSN1 in Table 2.
SaltWQ.glmssn1 <- glmssn(trout_100m ~ SLOPE + S1_93_11 + CANOPY, SaltWQ,
  CorModels = c("Exponential.tailup", "Exponential.taildown"),
  addfunccol = "afvArea", EstMeth = "REML")
summary(SaltWQ.glmssn1)

#Fit SSN2 in Table 2.
SaltWQ.glmssn2 <- glmssn(trout_100m ~ SLOPE + S1_93_11 + CANOPY, SaltWQ,
  CorModels = c("Exponential.tailup", "Exponential.taildown", "Exponential.Euclid"),
  addfunccol = "afvArea", EstMeth = "REML")
summary(SaltWQ.glmssn2)

#Fit SSN3 in Table 2.
SaltWQ.glmssn3 <- glmssn(trout_100m ~ S1_93_11, SaltWQ,
  CorModels = c("Exponential.tailup", "Exponential.taildown"),
  addfunccol = "afvArea", EstMeth = "REML")
summary(SaltWQ.glmssn3)

#Fit SSN4 in Table 2.
SaltWQ.glmssn4 <- glmssn(trout_100m ~ 1, SaltWQ,
  CorModels = c("Exponential.tailup", "Exponential.taildown"),
  addfunccol = "afvArea", EstMeth = "REML")
summary(SaltWQ.glmssn4)

```
#Fit SSN5 in Table 2.
SaltWQ.glmssn5 <- glmssn(trout_100m ~ 1, SaltWQ,
  CorModels = c("Exponential.tailup", "Exponential.taildown", "Exponential.Euclid"),
  addfunccol = "afvArea", EstMeth = "REML")
summary(SaltWQ.glmssn5)

#Report AIC values (Use ML instead of REML in above model fits to estimate correct AIC values)
AIC(SaltWQ.glmssn0)
AIC(SaltWQ.glmssn1)
AIC(SaltWQ.glmssn2)
AIC(SaltWQ.glmssn3)
AIC(SaltWQ.glmssn4)
AIC(SaltWQ.glmssn5)

#Report cross-validation statistics and confidence intervals
CrossValidationStatsSSN(SaltWQ.glmssn0)
CrossValidationStatsSSN(SaltWQ.glmssn1)
CrossValidationStatsSSN(SaltWQ.glmssn2)
CrossValidationStatsSSN(SaltWQ.glmssn3)
CrossValidationStatsSSN(SaltWQ.glmssn4)
CrossValidationStatsSSN(SaltWQ.glmssn5)

#Report variance composition among covariate effects and autocovariance functions
varcomp(SaltWQ.glmssn0)
varcomp(SaltWQ.glmssn1)
varcomp(SaltWQ.glmssn2)
varcomp(SaltWQ.glmssn3)
varcomp(SaltWQ.glmssn4)
varcomp(SaltWQ.glmssn5)

#Plot graphs of leave-one-out cross-validation (LOOCV) predictions & SEs
cv.out <- CrossValidationSSN(SaltWQ.glmssn2)
par(mfrow = c(1, 1))
plot(SaltWQ.glmssn2$sampinfo$z,
  cv.out[, "cv.pred"], pch = 19,
  xlab = "Observed Data", ylab = "LOOCV Prediction")

#Save LOOCV predictions & SEs to working directory file
write.csv(cv.out, "cv_out_trout100m.csv", row.names = FALSE)

#Calculate & plot model residuals & influence measures
resids <- residuals(SaltWQ.glmssn2)
class(resids)
resids.df <- getSSNdata.frame(resids)
names(resids.df)
plot(resids)
hist(resids, xlab = "Raw Residuals")
qqnorm(resids)

#Save residuals & influence measures to working directory file
```

```
write.csv(resids.df, "resids_trout100m.csv", row.names = FALSE)

#Plot 108 observation sites as large circles prior to block-kriging prediction points
plot(SaltWQ, "trout_100m", pch = 1, cex = 3,
    xlab = "x-coordinate (m)", ylab = "y-coordinate (m)",
    xlim = c(1715000,1770000), ylim = c(1370000,1450000))


#Plot 100m prediction points for individual stream blocks
SaltWQ.glmssn2.cottonwood <- predict(SaltWQ.glmssn2, "Cottonwood")
plot(SaltWQ.glmssn2.cottonwood, "trout_100m", add = TRUE,
    xlim = c(1715000,1770000), ylim = c(1370000,1450000))
SaltWQ.glmssn2.crow <- predict(SaltWQ.glmssn2, "Crow")
plot(SaltWQ.glmssn2.crow, "trout_100m", add = TRUE,
    xlim = c(1715000,1770000), ylim = c(1370000,1450000))
SaltWQ.glmssn2.dry <- predict(SaltWQ.glmssn2, "Dry")
plot(SaltWQ.glmssn2.dry, "trout_100m", add = TRUE,
    xlim = c(1715000,1770000), ylim = c(1370000,1450000))
SaltWQ.glmssn2.jackknife <- predict(SaltWQ.glmssn2, "Jackknife")
plot(SaltWQ.glmssn2.jackknife, "trout_100m", add = TRUE,
    xlim = c(1715000,1770000), ylim = c(1370000,1450000))
SaltWQ.glmssn2.salt <- predict(SaltWQ.glmssn2, "Salt")
plot(SaltWQ.glmssn2.salt, "trout_100m", add = TRUE,
    xlim = c(1715000,1770000), ylim = c(1370000,1450000))
SaltWQ.glmssn2.spring <- predict(SaltWQ.glmssn2, "Spring")
plot(SaltWQ.glmssn2.spring, "trout_100m", add = TRUE,
    xlim = c(1715000,1770000), ylim = c(1370000,1450000))
SaltWQ.glmssn2.strawberry <- predict(SaltWQ.glmssn2, "Strawberry")
plot(SaltWQ.glmssn2.strawberry, "trout_100m", add = TRUE,
    xlim = c(1715000,1770000), ylim = c(1370000,1450000))
SaltWQ.glmssn2.stump <- predict(SaltWQ.glmssn2, "Stump")
plot(SaltWQ.glmssn2.stump, "trout_100m", add = TRUE,
    xlim = c(1715000,1770000), ylim = c(1370000,1450000))
SaltWQ.glmssn2.swift <- predict(SaltWQ.glmssn2, "Swift")
plot(SaltWQ.glmssn2.swift, "trout_100m", add = TRUE,
    xlim = c(1715000,1770000), ylim = c(1370000,1450000))
SaltWQ.glmssn2.tincup <- predict(SaltWQ.glmssn2, "Tincup")
plot(SaltWQ.glmssn2.tincup, "trout_100m", add = TRUE,
    xlim = c(1715000,1770000), ylim = c(1370000,1450000))
SaltWQ.glmssn2.willow <- predict(SaltWQ.glmssn2, "Willow")
plot(SaltWQ.glmssn2.willow, "trout_100m", add = TRUE,
    xlim = c(1715000,1770000), ylim = c(1370000,1450000))
SaltWQ.glmssn2.saltriver <- predict(SaltWQ.glmssn2, "SaltRiver")
plot(SaltWQ.glmssn2.saltriver, "trout_100m", add = TRUE,
    xlim = c(1715000,1770000), ylim = c(1370000,1450000))

#Obtain block-kriging estimates of mean trout density & SEs for individual stream blocks
SaltWQ.glmssn2.cottonwood <- BlockPredict(SaltWQ.glmssn2, "Cottonwood")
SaltWQ.glmssn2.cottonwood
SaltWQ.glmssn2.crow <- BlockPredict(SaltWQ.glmssn2, "Crow")
SaltWQ.glmssn2.crow
```

SaltWQ.glmssn2.dry <- BlockPredict(SaltWQ.glmssn2, "Dry")
SaltWQ.glmssn2.dry
SaltWQ.glmssn2.jackknife <- BlockPredict(SaltWQ.glmssn2, "Jackknife")
SaltWQ.glmssn2.jackknife
SaltWQ.glmssn2.salt <- BlockPredict(SaltWQ.glmssn2, "Salt")
SaltWQ.glmssn2.salt
SaltWQ.glmssn2.spring <- BlockPredict(SaltWQ.glmssn2, "Spring")
SaltWQ.glmssn2.spring
SaltWQ.glmssn2.strawberry <- BlockPredict(SaltWQ.glmssn2, "Strawberry")
SaltWQ.glmssn2.strawberry
SaltWQ.glmssn2.stump <- BlockPredict(SaltWQ.glmssn2, "Stump")
SaltWQ.glmssn2.stump
SaltWQ.glmssn2.swift <- BlockPredict(SaltWQ.glmssn2, "Swift")
SaltWQ.glmssn2.swift
SaltWQ.glmssn2.tincup <- BlockPredict(SaltWQ.glmssn2, "Tincup")
SaltWQ.glmssn2.tincup
SaltWQ.glmssn2.willow <- BlockPredict(SaltWQ.glmssn2, "Willow")
SaltWQ.glmssn2.willow
SaltWQ.glmssn2.SaltRiver <- BlockPredict(SaltWQ.glmssn2, "SaltRiver")
SaltWQ.glmssn2.SaltRiver

#Save values of block predictions & SEs at 100m prediction points to working directory file
SaltWQ.cottonwood <- predict(SaltWQ.glmssn2, "Cottonwood")
pred1df <- getSSNdata.frame(SaltWQ.cottonwood, "Cottonwood")
write.csv(pred1df, "SaltWQ_trout100m_SSN2_cottonwood_BlockPredictions.csv", row.names = FALSE)

#Plot 100m prediction points for full network
SaltWQ.glmssn2.network <- predict(SaltWQ.glmssn2, "Network")
plot(SaltWQ.glmssn2.network, "trout_100m", add = TRUE,
  xlim = c(1715000,1770000), ylim = c(1370000,1450000))

#Obtain block-kriging estimates of mean trout density & SEs for full network (calculation requires several minutes)
SaltWQ.glmssn2.network <- BlockPredict(SaltWQ.glmssn2, "Network")
SaltWQ.glmssn2.network

#Plot predictions for full network at reach midpoints with symbol size inverse to SEs
SaltWQ.preds <- predict(SaltWQ.glmssn2, "preds")
*plot(SaltWQ.preds, SEcex.max = 1.4, SEcex.min = .7/3*2,*
  breaktype = "user", brks = brks)

#Is this cool or what?